A gas cell apparatus for measuring charge exchange cross sections with multicharged ions

S. J. Bromley, D. C. Fox, C. E. Sosolik, J. E. Harriss, and J. P. Marler

Citation: Review of Scientific Instruments **89**, 073107 (2018); doi: 10.1063/1.5028139
View online: https://doi.org/10.1063/1.5028139
View Table of Contents: http://aip.scitation.org/toc/rsi/89/7
Published by the American Institute of Physics

A gas cell apparatus for measuring charge exchange cross sections with multicharged ions

S. J. Bromley,[a] D. C. Fox, C. E. Sosolik, J. E. Harriss, and J. P. Marler[b]
Department of Physics and Astronomy, Clemson University, Clemson, South Carolina 29634, USA

(Received 7 March 2018; accepted 22 June 2018; published online 12 July 2018)

A gas cell apparatus to measure charge exchange cross sections for charge state- and energy-resolved ion beams with neutrals is described. The design features a short well-defined interaction region required for beams of multicharged ions with high cross sections. Our method includes measuring the beam transmission at four different neutral pressures and extracting the cross section from the slope of a beam loss vs pressure plot. The design and procedure were tested for Ar^+ interacting with neutral Ar gas over the incident ion energy range of 1.0–5.0 keV. The charge exchange cross sections agree well with previous complementary measurement techniques. *Published by AIP Publishing.* https://doi.org/10.1063/1.5028139

I. INTRODUCTION

Charge exchange is seen in a variety of environments, including fusion reactors,[1] solar wind,[2–5] planetary atmospheres,[6] and even extragalactic sources.[7] Charge exchange can be expressed as

$$A^{q+} + X \rightarrow A^{(q-j)+} + X^{j+}, \tag{1}$$

where a neutral atom X transfers j electrons to an ion, A^{q+}. The specific case of single charge exchange with singly charged ions (i.e., $q = j = 1$) is observed in many environments, ranging from Hall Effect Thrusters (HETs) to atmospheric plasmas. In HETs, the primary source of electronic erosion and solar panel failure arises from contamination of charge exchange ions, and understanding the charge exchange between fuel ions and neutrals has prompted a series of measurements on the cross sections of Xe^+ and Kr^+ propellants.[8,9] In the case of Earth's ionosphere, the ionization balance is strongly influenced by reactions of N^+ and O^+ ions interacting with their neutral surroundings.[10]

To understand the underlying dynamics of charge exchange, noble gas systems such as $Ar^+ + Ar$ studied here are some of the simplest experimentally accessible systems. In the case of Ar^+ on Ar, experimental results exist in the literature since the early 1950s and are in generally good agreement with the most recent results (see Ref. 11 and the references therein). However, there remain significant discrepancies in related systems of Ar^+ on the other noble gases. From a computational standpoint, methods exist for calculating a specific ion/target combination's cross sections directly (e.g., Refs. 12–14), but given the vast number of possible interesting combinations a drive to develop scaling relationships also continues.[15]

In the case of multicharged ions (MCIs) ($q > 1$), the transferred electron can be captured into an excited state of the ion (especially in the case of $q \gg 1$) and the charge exchange is inferred by the detection of a photon(s) from the relaxation process.[16] Laboratory observations of MCIs require an Electron Beam Ion Source (EBIS) or a similar apparatus.[17] Ideally, the source would deliver a pulse of a single charge state to an interaction region for further study. Additionally, the relatively large ($\approx 10^{-14} - 10^{-15}$ cm^2) charge exchange cross sections and low beam currents in multicharged ion sources require ultra-high vacuum conditions to prevent beam loss prior to arriving at the interaction region.[18] MCI-neutral reactions open up the possibility of multielectron transfer ($j > 1$), and accurate analysis requires diagnostic techniques such as a retarding field analyzer (RFA)[19] or Cold Target Recoil Ion Momentum Spectrometer (COLTRIMS)[20] to differentiate between final ion states. Additionally, in the case of molecular targets, one could include a correlated detection scheme to study charge exchange-induced fragmentation.

The Clemson University Electron Beam Ion Trap (CUEBIT) facility has recently gone online.[21] To benchmark a new gas cell for multicharged ion experiments, we use a singly charged ion source and measure the charge exchange cross section for $Ar^+ + Ar \rightarrow Ar + Ar^+$ for ion energies of 1–5 keV, which has a cross section ($\approx 10^{-15}$ cm^2) similar to what is found in MCI-neutral charge exchange.[11]

The gas cell presented in this paper has been designed to attach to the CUEBIT and will be implemented into an experimental program to systematically explore and understand charge exchange with MCIs. In Sec. II, we describe the apparatus and our technique to measure absolute charge exchange cross sections using relative pressure measurements. In Sec. III, we present energy-resolved cross sections for charge exchange between Ar^+ and neutral Ar and compare to other experimental measurements. In Sec. IV, we summarize our findings and propose future experiments utilizing the gas cell for measuring MCI-neutral cross sections.

II. EXPERIMENT

A. Apparatus

Our gas cell, shown in Figs. 1 and 2, was designed with consideration for future experiments with multicharged ions.

[a]Electronic mail: sjbroml@clemson.edu
[b]Electronic mail: jmarler@clemson.edu

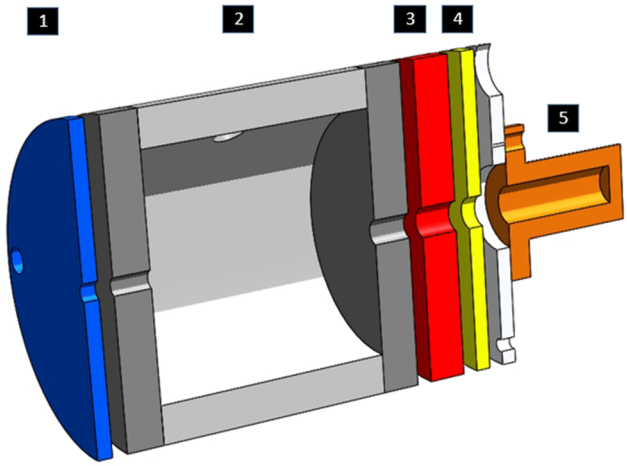

FIG. 1. Cross section of the gas cell components showing: 1. Faceplate (blue), 2. Gas cell (gray), 3. Retarding field analyzer (red), 4. Suppression electrode (yellow), and 5. Faraday cup (orange). For scale, the retarding field analyzer is 6.3 mm thick and has an outer diameter of 52 mm.

The large charge exchange cross sections for MCIs require the use of low gas pressures and/or short interaction path lengths to ensure only single collisions. In order to run with pressures $>10^{-5}$ mbar, the cell length was chosen so that the current loss from the beam would be on the order of 5%-10%. The gas cell body is a stainless steel cylinder 40 mm in length and internal diameter. Both entrance and exit endcaps are 6.3 mm thick with entrance and exit apertures of 3 and 4 mm, respectively. With this geometry, the effective path length is estimated to be 52.6 mm, to be discussed in more detail in Sec. III. The dimensions of the gas cell apertures provide a pressure ratio between the interaction region and the experimental chamber approaching 10^3.

The elements after the cell body include a retarding field analyzer (RFA), suppression electrode (SE), and Faraday cup (FC). All elements are isolated by MACOR® (MACOR is a registered trademark of Corning Incorporated, Corning, NY.) top hat washers on two #5-40 rods that thread into the cell body. The RFA plate is 6.3 mm thick with a 5 mm aperture.

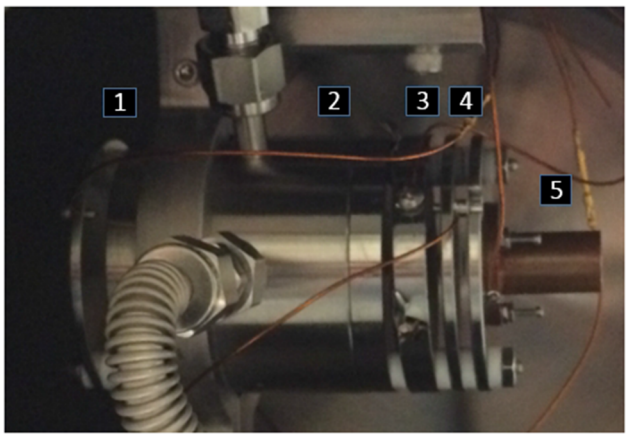

FIG. 2. Photograph of the gas cell showing the five major electrical components, gas connections, and supporting bracket. Numbered components follow the same convention as Fig. 1.

The dimensions of the copper FC (6.3 mm internal diameter by 20 mm depth) ensure a small diameter-to-length aspect ratio of 0.3 and were chosen to minimize the error due to secondary electrons. Faraday cup currents were fed through a current-to-voltage converter before being measured by a multimeter. Electron suppression was provided by a thin (2.5 mm thick) suppression electrode mounted between the RFA and the FC. For these results, the suppression voltage was held at −120 V.

In a different configuration, this RFA and FC were used previously to show that the kinetic energy spread of MCI beams produced in the CUEBIT had a full-width at half-maximum (FWHM) of 20 eV.[22] To aid the alignment of the gas cell with the incident ion beam, the apparatus is mounted on a vertical rod suspended from a UHV manipulator that provides translation in 3 dimensions and 360 degrees of rotation. The current on the faceplate (FP) is continuously monitored by an ammeter and used as an indicator of ion source stability over the course of a measurement.

The vacuum system houses three pressure gauges: two Pfeiffer Full-Range Cold Cathode (PKR 251) gauges mounted inside and directly outside the ion source and one Pfeiffer Bayard-Alpert (BA) Full-Range (PBR 260) gauge connected to the gas cell by approximately 350 mm of 6.3 mm flexible stainless steel bellows. The hot BA gauge was chosen for the Ar pressure measurement in the cell due to the presence of an "argon instability" noticed with the cold cathode gauges.[23] Neutral pressures in the cell were measured directly with the Bayard-Alpert gauge. The measured neutral pressure in the cell was corrected for Ar using the mean correction factor provided by the manufacturer, $P_{\mathrm{Ar}} = 0.8 \times P_{\mathrm{measured}}$. Base pressures in the system were 5×10^{-8} mbar in the UHV chamber and 3×10^{-7} mbar in both the gas cell and ion source prior to gas injection. LabVIEW was used to monitor all currents and pressures during data collection.

To benchmark the capabilities of the gas cell, the reaction $Ar^+ + Ar \rightarrow Ar + Ar^+$ was chosen as the charge exchange cross section is within an order of magnitude of typical MCI-neutral cross sections ($\approx 10^{-15}$ cm^2). The first data collected with the cell used a singly charged ion source (OMICRON ISE 10 sputter ion source) capable of producing 20 μA of Ar^+ at energies up to 5 keV. For these experiments, ultra-high purity Ar was injected by a leak valve into the ion source region such that the Ar pressure was on the order of 2-5 $\times$ 10^{-4} mbar. To minimize gas flow between the ion source and gas cell, the ion source was mounted approximately 370 mm from the FP. At this pressure and for ions extracted with 5 keV energy, typical beam currents were 6000 and 60 nA measured with the FP and FC, respectively. Calibration of the ion beam energy was obtained by scanning the RFA voltage through each beam energy of interest. Fitting Gaussian profiles to the derivative of the FC current as a function of RFA voltage, we find good agreement with the selected energies on the source controller and a FWHM ($\approx$25 eV) much less than our energy step size of 250 eV. The RFA was grounded for the measurements presented in Sec. III.

B. Method

The charge exchange cross section can be found by comparing the rate of neutralization to the fraction of ion beam current lost by passage through the neutral gas,

$$\frac{dI}{dz} = -In\sigma_{\mathrm{cx}}, \tag{2}$$

where I is the ion beam current as a function of path length, n is the number density of the target gas, σ_{cx} is the charge exchange cross section, and z is the distance along the axis of the cell. Rearranging Eq. (2) and integrating over the path length (L) give

$$I(L) = I_o e^{-Ln\sigma_{\mathrm{cx}}}. \tag{3}$$

We assume that the neutral pressure is low enough that the target gas behaves ideally, where $PV = Nk_bT$. Using the Taylor expansion $e^{-x} = \sum_{n=0}^{\infty} \frac{(-x)^n}{n!}$ and truncating the sum for thin targets ($e^{-x} \approx 1 - x$), Eq. (3) simplifies to

$$\sigma_{\mathrm{cx}} = \frac{k_bT}{PL}\left(\frac{I_o - I}{I_o}\right), \tag{4}$$

where k_b is the Boltzmann constant, T is the absolute temperature of the gas, and P is the neutral pressure in the gas cell. L is the effective path length of the interaction region, I_o is the current in the FC with no gas in the cell, and I is the current measured with gas in the cell. Solving Eq. (4) for the fractional loss of ions from the beam, we find

$$\left(\frac{I_o - I}{I_o}\right) = P\,\frac{L\,\sigma_{\mathrm{cx}}}{k_bT}. \tag{5}$$

Using Eq. (5), the cross section is found from the slope $= \frac{L\sigma_{\mathrm{cx}}}{k_bT}$ of a linear fit to the percent current loss at each energy as a function of pressure in the cell. The linearity of the percent current loss as a function of pressure is indicative that the measurements are in the single collision regime.

Starting with an empty gas cell, we optimize the extraction and focusing voltages for each beam energy to produce the maximum I_0 in the FC. I_0 was recorded at each beam energy, and neutral Ar gas was introduced into the cell through a UHV leak valve and 550 mm of oxygen-free copper tubing mounted inside the UHV manipulator. A measure of I was then obtained at each beam energy of interest. Gas was further introduced for four different cell pressures between 1×10^{-4} and 7×10^{-4} mbar to ensure molecular flow conditions. The entire above procedure was repeated 4 times, and the measured cross sections, extracted from the slope of the linear fits, are the average of the 4 scans. A sample plot of percent current loss is shown in Fig. 3 for 1 and 5 keV beams.

III. RESULTS

Our results for the $Ar^+ + Ar \rightarrow Ar + Ar^+$ charge exchange cross section are plotted in Fig. 4 along with measurements from the most recent other work.[11] The error bars shown in Fig. 4 are the standard deviation of four measurements at each beam energy of interest. The current results are consistent (both in shape and absolute value) with the work of Martinez *et al.* that measured differential cross sections and integrated for the total cross section. Our trend for a decrease in σ_{cx} with increasing ion energy is consistent with the trends found in previous experimental[11] and theoretical[12] studies on $Ar^+ + Ar$. In general, the probability for charge exchange is proportional to the time spent in close proximity between the target and projectile and hence inversely proportional to the ion energy.[24]

The RFA was held at 0 V for the present measurements, so inelastic collisions (i.e., electronic excitation, ionization without charge exchange) will not affect our collected current. The maximum scattering angle that will still result in ions collected at the FC ranges from 2° for collisions at the front of the gas cell body to 13° for collisions near the exit of the gas cell body. Previous studies have shown that elastic scatter in symmetric reactions at these energies is primarily in the forward direction with the cross section falling off by almost an order of

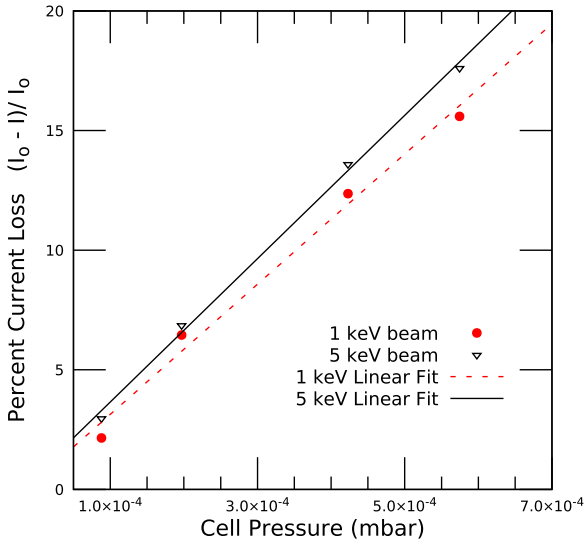

FIG. 3. Percent current loss of the ion beam at 1 keV (red circles) and 5 keV (open triangles) ion beam energies.

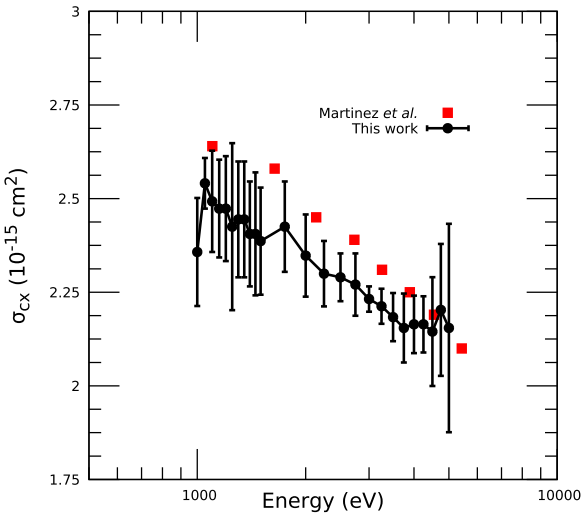

FIG. 4. Charge exchange cross section for $Ar^+ + Ar \rightarrow Ar + Ar^+$ with ion energies between 1.0 and 5.0 keV for this work (black) and that of Martinez *et al.*[11] (red). The error bars shown represent statistical uncertainty in the measurements. The systematic uncertainty is estimated at ± 17%.

magnitude by 2°.[25,26] While scattering at angles greater than these angles would contribute to the measured charge exchange cross section, these are expected to be small for the ion beam energies studied.[25]

The charge exchange cross section was calculated from the slope of the current loss vs pressure plot. This method eliminates any additive shift from the measured gauge pressure (e.g., from constant non-zero background gas pressure). However, there are other uncertainties associated with the cross section. The absolute pressure measurement has an accuracy of 15% according to the manufacturer.

Another source of uncertainty is the effective path length for the interaction region. Previous calculations estimate that for thin-walled large cylinders with diameter ≈ L, the path length experienced by the beam is close to the length of the cell body.[27] Other experimental studies with a gas cell with thin endcaps suggest that the path length of the cell is closer to the sum of the cell length and aperture radii.[28] Here we assume that each of the thick entrance and exit endcaps contributes 6.3 mm to the total path length of 52.6 mm. The cross sections calculated under this assumption (Fig. 4) agree well with the previous measurements of Martinez *et al.*, which utilized a different design and technique.[11] However, we follow the convention of Greenwood *et al.* and assume a large uncertainty in the path length equal to the sum of the exit and entrance aperture radii (7%).[28]

The target gas and apparatus used here are in equilibrium with the ambient room temperature measured to be 24 °C. The temperature in the room is stable to within ± 1 °C according to the measurements over a day. Thus, we may attribute an additional 0.5% uncertainty (1 K/298 K) in the cross sections from uncertainty in the gas temperature.

Given the distance from the ion source to the gas cell and the large pressure differential between the cell and the chamber during gas injection, we estimate at most a 2% uncertainty in I_o resulting from beam attenuation outside the cell. Over the course of a measurement, a drift in ion source pressure results in a slight change in the ion beam current as measured by the FP. This contributes an additional 3% uncertainty in the cross section, derived from the largest deviation in ion beam current measured on the cell faceplate during a typical measurement. Accounting for these contributions, including noise in the amplifier (1%) and uncertainty in the measurement of the FC currents (1%), we find a total uncertainty in σ_{cx} of 17% which is double the average statistical uncertainty found in Fig. 4.

IV. SUMMARY

A gas cell apparatus for measuring absolute charge exchange cross sections of multicharged ions and neutrals was described. The dimensions of the gas cell support a large pressure ratio ($\approx 10^3$) between the interaction region and vacuum chamber during gas injection that minimizes the uncertainty in the path length experienced by the ion beam. To aid in alignment with the MCI beam produced in the CUEBIT, the cell is supported in a UHV manipulator for rotation and 3-dimensional translation. We demonstrated the measurement capabilities of the cell and method using a well-studied reaction with a cross section comparable ($\approx 10^{-14} - 10^{-15}$ cm^2) to those found in MCI-neutral charge exchange. Using both the singly charged ion source and the CUEBIT, future experiments will carry out a systematic survey of both symmetric ($A^{q+} + A \rightarrow A^{(q-j)+} + A^{j+}$) and asymmetric ($A^{q+} + X \rightarrow A^{(q-j)+} + X^{j+}$) charge exchange involving noble gas ions down to energies of 100's of eV/q.

ACKNOWLEDGMENTS

The authors gratefully acknowledge the work of the Physics and Astronomy Instrumentation Shop and financial support from the Clemson University College of Science.

[1] R. Janev, M. Harrison, and H. Drawin, Nucl. Fusion **29**, 109 (1989).
[2] N. A. Schwadron and T. E. Cravens, Astrophys. J. **544**, 558 (2000).
[3] R. J. Mawhorter, A. Chutjian, T. E. Cravens, N. Djurić, S. Hossain, C. M. Lisse, J. A. MacAskill, S. J. Smith, J. Simcic, and I. D. Williams, Phys. Rev. A **75**, 032704 (2007).
[4] A. Bhardwaj, M. B. Dhanya, A. Alok, S. Barabash, M. Wieser, Y. Futaana, P. Wurz, A. Vorburger, M. Holmström, C. Lue, Y. Harada, and K. Asamura, Geosci. Lett. **2**, 10 (2015).
[5] P. D. Mullen, R. S. Cumbee, D. Lyons, L. Gu, J. Kaastra, R. L. Shelton, and P. C. Stancil, Astrophys. J. **844**, 7 (2017).
[6] M. Larsson, W. D. Geppert, and G. Nyman, Rep. Prog. Phys. **75**, 066901 (2012).
[7] A. C. Fabian, J. S. Sanders, R. J. R. Williams, A. Lazarian, G. J. Ferland, and R. M. Johnstone, Mon. Not. R. Astron. Soc. **417**, 172 (2011).
[8] J. S. Miller, H. S. Pullins, D. J. Levandier, Y. Chiu, and R. A. Dressler, J. Appl. Phys. **91**, 984 (2002).
[9] M. Hause, B. Prince, and R. Bemish, J. Appl. Phys. **113**, 163301 (2013).
[10] R. G. Roble and C. C. Ridley, Annales Geophys. **5A**, 369 (1987).
[11] H. Martinez, F. Castillo, P. Reyes, and F. Santibañez, Int. J. Mass Spectrom. **228**, 107 (2003).
[12] D. Rapp and D. E. Francis, J. Chem. Phys. **37**, 2631 (1962).
[13] F. Sattin, Phys. Rev. A **64**, 034704 (2001).
[14] B. Friedman and D. Larson, Phys. Rev. A **91**, 022710 (2015).
[15] B. Friedman and G. DuCharme, J. Phys B: At., Mol. Opt. Phys. **50**, 115202 (2017).
[16] M. Fogle, D. Wulf, K. Morgan, D. McCammon, D. G. Seely, I. N. Draganic, and C. C. Havener, Phys. Rev. A **89**, 042705 (2014).
[17] G. Zschornack, V. P. Ovysannikov, F. Grossman, A. Schawn, and F. Ullmann, J. Instrum. **5**, C08012 (2010).
[18] T. Kusakabe, Y. Miyamoto, R. Ishida, K. Itoh, N. Kuroyanagi, Y. Nakai, and T. Shirai, Nucl. Instrum. Methods Phys. Res., Sect. B **205**, 600 (2003).
[19] J. Vancura, V. J. Marchetti, J. J. Perotti, and V. O. Kostroun, Phys. Rev. A **47**, 3758 (1993).
[20] R. Ali, AIP Conf. Proc. **926**, 216 (2007).
[21] R. Shyam, D. D. Kulkarni, D. A. Field, E. S. Srinadhu, D. B. Cutshall, W. R. Harrell, J. E. Harriss, and C. E. Sosolik, AIP Conf. Proc. **1640**, 129 (2015).
[22] D. D. Kulkarni, C. D. Ahl, A. M. Shore, A. J. Miller, J. E. Harriss, C. E. Sosolik, and J. P. Marler, Rev. Sci. Instrum. **88**, 083306 (2017).
[23] T. Tom and B. D. James, J. Vac. Sci. Technol. **6**, 304 (1969).
[24] B. G. Lindsay and R. F. Stebbings, J. Geophys. Res. **110**, A12213, https://doi.org/10.1029/2004ja010854 (2005).
[25] W. Aberth and D. C. Lorents, Phys. Rev. **144**, 109 (1966).
[26] V. Sidis, M. Barat, and D. Dhuicq, J. Phys B: At., Mol. Opt. Phys. **8**, 474 (1975).
[27] B. P. Mathur, J. E. Field, and S. O. Colgate, Phys. Rev. A **11**, 830 (1975).
[28] J. B. Greenwood, I. D. Williams, S. J. Smith, and A. Chutjian, Phys. Rev. A **63**, 062707 (2001).